Energy 313 (2024) 133713

Contents lists available at ScienceDirect

Energy

journal homepage: www.elsevier.com/locate/energy

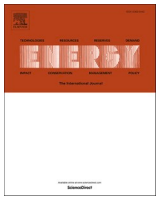

Experimental evaluation of the CO_2-based mixture CO_2/C_6F_6 in a recuperated transcritical cycle

Viktoria Carmen Illyés [a,*], Gioele Di Marcoberardino [b], Andreas Werner [a], Markus Haider [a], Giampaolo Manzolini [c]

[a] TU Wien, Institute for Energy Systems and Thermodynamics, Getreidemarkt 9, 1060, Wien, Austria
[b] Dipartimento di Ingegneria Meccanica ed Industriale, Università degli Studi di Brescia, Via Branze 38, 25123, Brescia, Italy
[c] Energy Department, Politecnico di Milano, 20156, Milano, Italy

ARTICLE INFO

Keywords:
Zeotropic working fluid
CO2-Based power cycle
Composition shift
Rankine cycle

ABSTRACT

Zeotropic CO_2-based mixtures as working fluids in the power block have the potential to enhance concentrated solar power (CSP) plants and other high-temperature heat source applications. One promising working fluid is the CO_2/C_6F_6 mixture, which enables condensation at 50 °C – a necessity when dry cooling with ambient air. Given the many theoretical studies on topics such as potential, optimized performance, or economic assessments, an experimental validation and a reality-check in a facility of significant size is required to vindicate further research. The experimental campaign was performed on pure CO_2 and the CO_2/C_6F_6 mixture in two compositions in a test facility (recuperated transcritical cycle). The long-term test (170h) revealed no operational issues, including no signs of thermal degradation. However, a composition shift - an effect previously regarded as an issue in closed cycles with zeotropic mixtures - affected the conditions at the vapor-liquid-equilibrium in the systems tank but also self-stabilizes the system to remain condensing, even at higher ambient air temperatures. The successful proof-of-concept at cycle temperatures of up to 500 °C – significantly higher than earlier studies on mixtures reported (<300 °C) – justifies further research in this area.

1. Introduction

Supercritical carbon dioxide (sCO_2) power cycles have been identified as one of the key enabling technologies for the 3rd generation of concentrated solar power (CSP) with temperatures of 700 °C and higher [1]. The sCO_2 power cycle's thermal efficiency surpasses that of the traditional steam Rankine cycle at high maximum cycle temperatures (turbine inlet temperatures) of >470–650 °C while maintaining a simple Brayton layout of great compactness [2]. However, the advantage in terms of conversion efficiency strongly reduces at high condensing temperatures (above 40 °C) as the compressor does not operate in its most favorable conditions [3]: this is the typical situation of CSP plants which operate in arid and hot environments; dry-cooling therefore minimizes water consumption [4].

Adding a second component to the CO_2 into a binary mixture can alter the properties of the resulting working fluid by shifting the critical point to higher temperatures [5], thus shifting the whole two-phase dome, making condensation possible even at higher temperatures [6].

Apart from power generation, mixtures as working fluids have been investigated in refrigeration cycles, and heat pump cycles [7,8]. CO_2-mixtures have also been studied for heat pumps, mixed with other refrigerants, such as R32, R143a and R41 [9]. Their use in power cycles is the most recent in this respect, and requires dedicated investigation on the account of the completely different operating ranges. Sandia National Laboratories have performed some experiments for geothermal applications (maximum temperature up to 200 °C) demonstrating the validity of the concept [10].

Fig. 1 shows the application fields of mixture power cycles for low, medium, and high temperatures. Most commonly, the (subcritical) organic Rankine cycle and the Kalina cycle are applied for low-temperature heat sources, solar, geothermal or waste heat recovery [11], where the high share of economization heat and dry expansion provides benefits with respect to steam Rankine cycles. Ocean thermal energy conversion, at very low heat source temperatures [18], and, sometimes even lower heat sink temperatures down to −162 °C using LNG cold energy recovery, is a potential application of zeotropic

* Corresponding author.
E-mail address: viktoria.illyes@tuwien.ac.at (V.C. Illyés).

https://doi.org/10.1016/j.energy.2024.133713
Received 23 August 2024; Received in revised form 19 October 2024; Accepted 3 November 2024
Available online 5 November 2024

mixtures with CO_2-based working fluids [19].

A relatively new concept is zeotropic mixtures based on supercritical CO_2 in power cycles of a high-temperature heat source such as CSP [12]. Researchers at the EU-funded project SCARABEUS have evaluated a wide range of second components to fit the application's specific needs. Three reoccur: hexafluorobenzene C_6F_6 [13], titanium tetracloride $TiCl_4$ [3], and sulfur dioxide SO_2 [14]. Simulations yield the following results for the utilization of CO_2-based mixtures.

- Two more design parameters have to be considered when compared to a pure CO_2 cycle: (1) selection of the second component and (2) its concentration (composition of the mixture) [15]. These additional options lead to different optimal cycle layouts with respect to the most beneficial ones for sCO_2. Based on maximizing the thermal efficiency at 700 °C maximum and 50 °C minimum cycle temperature, Crespi et al. [13] found the recuperated Rankine cycle working on $CO_2/TiCl_4$ and the Recompression cycle working on CO_2/SO_2, best performing with thermal efficiencies of 52.0 % and 51.2 %. Meanwhile, the optimized pure CO_2 cycle with a recompression layout achieves 49.5 % at 700 °C. At lower maximum temperatures of 550 °C, the precompression layout working on CO_2/C_6F_6 is the most interesting solution.
- The thermal efficiency of sCO_2-based mixtures exceeds the performance of state-of-the-art steam Rankine cycles and the sCO_2 cycle equivalent when optimized [3]. The efficiency gain can be as high as 5 % points.
- As the thermodynamic advantages of the sCO_2-based mixture power cycle strengthen with an increasing ambient/heat rejection temperature, the technology seems an excellent fit for the 3rd CSP generation. The first techno-economic analysis suggests a cost reduction when compared to (pure) sCO_2 technology [16].

However, inaccurate property calculation might suspend optimization efforts – an issue that also arose in zeotropic ORC cycles – and makes experimental validation of the accuracy of property calculation necessary. Di Marcoberardino et al. [17] studied the influence of equations of state on the performance of the CO_2/C_6F_6 power cycle. They found a difference of 1 % point in the cycle performance although the optimal composition of the best performing cycles per equation of state ranged between 81 and 87 % molar fraction CO_2. Such a deviation affects the cycle components' design and highlights the necessity of thoroughly evaluating the mixture properties.

To summarize, several modelling activities have shown the potential of CO_2-based mixtures in power conversion, but no experimental results of cycle operation at temperature above 300 °C have been recorded so far.

In this study, we present the results of the recuperated Rankine cycle with an expansion valve operating with pure CO_2 and mixtures of CO_2/C_6F_6 in compositions of 98.3 %/1.7 % and 93.8 %/6.2 % (molar fractions) proving the feasibility of such a system at a relevant size. This will be the first results for a power generation cycle utilizing mixtures at medium-high temperatures above 300 °C. The experimental campaign addresses the following open research questions: Does the mixture operate under stable conditions over time? Is the composition constant or is there any composition shift because of the different volatility during operation, an issue theoretically known from other mixture cycles? What is the impact of the mixture composition on the test facility operation? The following sections will summarize the research gaps and how the experimental campaign answers these questions.

2. Previous work

Azeotropic mixtures emerged in the 1950's as working fluids in refrigeration cycles [7] but can be treated like pure substances regarding their phase change. Due to their non-isothermal condensation and evaporation, zeotropic mixtures experience a temperature glide during phase change processes. The matching of working fluid and heat source/sink leads to a parallel temperature distribution between the fluids in heat exchangers, which in turn leads to better thermodynamic performances of thermodynamic cycles.

Zeotropic mixtures were first studied for heat pumps in the 1980s, resulting in mixtures such as R-410A [20], which is now among the most used refrigerants in air-conditioning (although they will be phased out due to their high GWPs) and are considered as fourth-generation refrigerants [21]. One of the first mixture power generation cycles, published in 1984, was a modified Rankine cycle – the Kalina cycle - using a water/ammonia mixture for a low-temperature heat source [22]. Mixture ORCs stem from around the same time (80s–90s) [23], [24], even under the consideration of supercritical conditions [25].

2.1. Experimental work on power cycles with zeotropic mixtures

Theoretical studies of a wide range of zeotropic mixture working fluids for ORCs concentrate on thermal efficiency and exergy analyses. The results reveal that the selection is a matter of fitting the fluid to the available operating conditions, particularly to the heat source and heat rejection. Only a handful of experimental works have been published: Abadi and Kim [26] cite four sources in their 2017 review, and a few more studies have been published since then, as shown in Table 1. Although no general approach for selecting a mixture fits all applications, there are trends in the experimentally tested mixtures: Many of the tested mixtures feature at least one of the common refrigerants, and all studies conducted are for low to low-medium temperatures.

The following issues were identified based on a recent review by Abadi and Kim [26] and the references in Table 1.

- Composition shift and fractionating of mixtures, resulting in a different circulating flow composition than the filling composition, must be accounted for during design as this might decrease the system's thermal efficiency.
- Reliable thermodynamic properties are not available for the majority of mixtures.

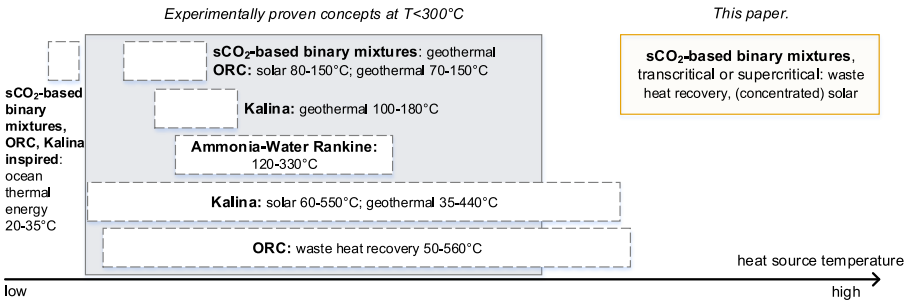

Fig. 1. Fields of application of zeotropic mixtures for power generation per hot source temperature level.

Table 1
Overview of experimental work on zeotropic mixtures in ORCs. Values in brackets for the maximum cycle temperature are estimations based on the heat source temperature.

Authors	Ref.	Year	Application	Max. cycle T	Pure Fluid	Mixture
Wang et al.	[28]	2010	Low-T solar	106 °C	R245fa	R245fa/R152a
Jung et al.	[29]	2015	medium-T WHR	136.4 °C	–	R245fa/R365mfc
Li et al.	[30]	2015	Low-T geothermal	(<110 °C)	R245fa	R245fa/R601a
Abadi et al.	[31]	2015	Low-T solar	113 °C	R245fa	R245fa/R134a
Wang et al.	[32]	2017	Low-T	104 °C	R601a	R601a/R600a
Blondel et al.	[33]	2019	Low-T WHR		NovecTM649	NovecTM649/HFE7000
Cai et al.	[34]	2020	Low-medium-T	(<110 °C)	–	R134a/R245fa
Huang et al.	[35]	2023	Low-medium-T	(<300 °C)	–	R134a/R245fa
Lu et al.	[36]	2023	Low-medium-T	(<300 °C)	–	R134a/R245fa
Wang et al.	[37]	2023	Low-T	(<100 °C)	R245fa, R141b	R245fa/R141b

- Heat transfer of mixtures is different from that of pure fluids, often deteriorated, and therefore has to be investigated specifically.
- The mixture components tested often have high Global Warming Potentials (1430 for R134a, 1030 for R245fa [27]) and will eventually be or are already banned by legislation in the EU, the USA, and some other countries.

For a low-temperature geothermal application, CO_2-based binary mixtures were proposed, and three mixtures of CO_2 with neon, SF_6, and butane were experimentally tested [10]. In the optimal cycle, a modified recompression Brayton cycle, Conboy et al. [10] found a 3.6 percentage points higher cycle efficiency for a 10 mol% butane CO_2-based mixture (18.1 %) than in the same cycle with pure CO_2 (14.5 %). It is unclear whether a higher efficiency is also achievable when comparing the mixture cycle against an optimized pure CO_2 cycle. However, the proposed cycle rejects heat at 46.7 °C by dry cooling.

Shu et al. [38] present CO_2-based mixture transcritical power cycles for the waste heat recovery of heavy duty-diesel (truck) engines. Experimental data for the mixture CO_2/R134a in a proportion of 0.7/0.3 validate their dynamic Simulink model. They examined the components of the cycle in off-design conditions and conclude that the finite volume method and moving boundary method model the heat exchangers sufficiently. They found that the dynamic response time of the system increases with the fraction of the refrigerant.

The EU-funded project Desolination is developing an optimized power cycle for a desalination system [39]. A demonstration is planned: The project team are preparing for the operation of their supercritical CO_2 test loop with a CO_2/SO_2 mixture of 25 % and 40 % molar fraction SO2 by setting up a dynamic model [40]. They predict that the heat exchangers and compressors should not face major shortcomings in capacity when operated in off-design with a mixture working fluid.

2.2. Composition shift and fractionating

Composition shift denotes that the composition of the circulating fluid in operation is different from the filling composition (sometimes also referred to as “charge”, “original”, or “bulk” composition). Fractionating describes the tendency to a particular composition variation in a system with gas and liquid phases. The vapor-liquid equilibrium in a system with a (for example, binary) mixture in two-phase conditions will result in a vapor phase comprising a higher degree of the higher volatile (low boiling point) component, which in our case is CO_2 for any additive. The liquid phase will have more of the lower volatile (high boiling point) component. Therefore, in our investigated mixture, the circulating flow composition will have a lower CO_2 fraction (and a higher additive fraction) than filling as a part of CO_2 is bound in the vapor phase of the cycle.

In a closed thermodynamic cycle, a composition shift occurs during the change of conditions at heat rejection: At lower cooling duties, temperature, and pressure rise while the composition of circulation fluids changes towards the lower volatile (high boiling point) component. Such heat rejection changes must be considered when using ambient air as a coolant.

Investigations of refrigeration and heat pump cycles have identified the holdup of working fluid in the two-phase flow heat exchangers (evaporators and condensers) as a significant contributor to composition shift [41]. The heat exchangers collect liquid with a higher concentration in the lower volatile (high boiling point) component and change the circulating fluid’s composition. Differential solubility of the components in the compressor oil was reported to affect the composition only minimally [41].

Zhao and Bao [42] recently showed a significant performance loss caused by composition shift with theoretical investigations on zeotropic mixture power cycles, in this case, an ORC. The validation of their simulation depends on experimental data of the composition shift during evaporation in a heat exchanger [43] due to a lack of composition shift data for (ORC) cycles.

To prevent the composition shift, a previous study suggested limiting the temperature glide between 5 and 15K [24] so that the vapor and liquid phase compositions will not differ much. However, the CO_2 blend considered in present study does not meet this criterion: The temperature glide can be as high as 88.4K (at 77.5 bar) for a CO_2/C_6F_6 mixture of 15 % molar fraction C_6F_6 as proposed in Ref. [13].

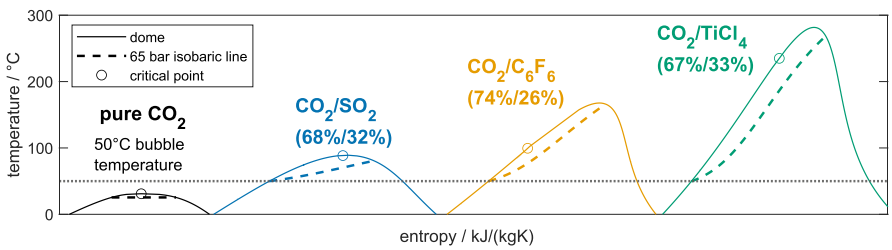

Fig. 2. T,s-diagram of three possible sCO_2-based mixtures in comparison to pure CO_2. This diagram shows compositions where the liquid fluid is saturated at 50 °C and 65 bar. For pure CO_2, the condensation temperature is 25.43 °C at 65 bar. The position of the critical temperature is an estimation.

Table 2
Suitability matrix for selecting from three possible second components for testing in the facility. + suitable, (+) acceptable, ? inconclusive data, - unsuitable.

	C_6F_6	SO_2	$TiCl_4$
High critical temperature	+, 244 °C [45]	+, 157.6 °C [46]	+, 366.0 °C [47]
Thermal stability up to 550 °C	+, up to 600 °C [48]	+, up to 2000 °C [49]	+
Thermal stability up to 700 °C	– [48]	?,[a]	?,[a]
Low toxicity, flammability and reactivity	+	–	–
Environmental impact	+	(+)	(+)
Cost effectiveness	(+)	+	+

[a] A mismatch between results obtained by University of Brescia and from the literature lead to the hypothesis that the pairing of material of the test pressure vessel and the contained component influences the thermal stability.

3. Methods

3.1. Working fluid selection

The immediate desired property change when employing a CO_2-based mixture instead of pure CO_2 is the higher critical temperature, leading to higher condensation temperatures that could be met by dry-cooling with air in warm environments suitable for concentrated solar power. The thermal stability of the component is another immediate requirement for the second component: Crespi et al. [3] concluded that the proposed cycle is competitive against steam cycles at maximum cycle temperatures higher than 550 °C in terms of thermal efficiency. A prerequisite for the binary mixture is the full solubility of the components (at desired conditions).

A survey of the literature identified three components as meeting the above-mentioned minimum requirements: hexafluorobenzene (C_6F_6), sulfur dioxide (SO_2), and ($TiCl_4$). Their T,s-diagrams of compositions, where condensation finishes at 50 °C and 65 bar, are shown in Fig. 2. These compositions illustrate the freedom in choosing the working fluid but careful optimization is necessary to find the ideal concentration of the mixture. Operating conditions in the design-point and off-design conditions and the cycle layout play a crucial role in this design process [44].

Alongside the thermodynamic aspects, the feasibility of a new working fluid depends on other criteria, such as safety, environmental impact, and cost/availability, categories where water/steam and pure CO_2 score highly.

Table 2 shows a matrix of the suitability of the three identified second components for testing in the facility. This oversimplified approach does not cover the nuances nor other desirable thermodynamic properties used to find an optimized working fluid but highlights the decision process for choosing our mixture. None of the three components meets all of the requirements.

Exposure to SO_2 poses serious health risks (increased risk of all-cause and respiratory mortality) even in low concentrations, with no clear threshold [50]. The Austrian (location of the test facility) government allows a daily mean of 0.5 ppm and a short-term (<15min) exposure of 1 ppm (mean value) up to 4 times per day according to their protective law for employees [51].

$TiCl_4$ is highly toxic, corrosive, and reactive with water (even with air humidity) producing hydrochloric acid and is commonly described as "most hazardous (worst 10 %) to human health" [52]. The additional safety installations necessary for handling these components in significant quantities are unreasonable for the laboratory scale on the one hand and are questionable on the industrial scale, especially when – compared to the conventional water/steam or pure CO_2 systems – the efficiency gain of the power block remains in the low percentage points. Because $TiCl_4$ hydrolyses quickly, it does not have a significant impact on the environment although the hydrolysis product hydrochloric acid has, if it does not dissociate in water. The inert hydrolysis product titanium dioxide might accumulate in soil and sediments [53].

Table 3
Compositions of tested working fluids.

	molar fraction/ CO_2/C_6F_6	mass fraction C_6F_6/-	total mass C_6F_6/kg	uncertainty molar fraction C_6F_6/-
Pure CO_2	100 %/0 %	0 %	0	0
MX1.7 %	98.3 %/1.7 %	7.0 %	7.9	±0.05 %
MX6.2 %	93.8 %/6.2 %	21.9 %	31.7	±0.18 %

Hexafluorobenzene is suitable in view of its low toxicity, flammability and reactivity but has the disadvantage of being flammable [54]. Although it causes eye and skin irritation, it is easy to handle because C_6F_6 is liquid under ambient conditions. However, in the mixture with CO_2, one of the recommended extinguishing materials, it is expected to be safe in the absence of oxygen and water, which might lead to degradation products such as CO and HF. The environmental impact is acceptable, according to the Scientific Assessment of Ozone Depletion 2022 [55], C_6F_6 has a global warming potential of 9. Moderate critical pressures of the pure component, ideally lower than the 73.8 bar of pure CO_2, avoid increasing costs by high operating pressures. C_6F_6's high critical temperature of 24 °C lies well above pure CO_2 (31 °C) while the critical pressure is lower at 32.8 bar compared to 73 bar. Hexafluorobenzene is stable up to temperatures of 600 °C when paired with Inconel 625 [48]. A price of 290€ per kilogram makes the component expensive [56], at least in the current market purchasing amounts in the range of 10–50 kg.

For these reasons, we chose to test C_6F_6 in two compositions. Due to C_6F_6's high cost, the lowest possible amounts for the low and high concentration compositions were chosen. For the low concentrations, the difference of the mixtures bubble line and CO_2's saturation line should be higher than 3K, well above the measurement accuracy. For the high concentrations, the saturation pressure at the highest condensation temperature (50 °C) to be tested at the low-pressure side should not exceed the design pressure of 100 bar. The resulting compositions are reported in Table 3.

The filling procedure contains three steps, first, flushing the system twice with pure CO_2, then, filling the liquid hexafluorobenzene per funnel at ambient conditions, and finally, applying pressure via CO_2 from liquid-filled gas bottles. The amount of filled components is weighed. A pressure difference between the gas bottles and the facility, both in vapor-liquid conditions after filling the first few kilograms, is created by operating the condensers at full capacity, reaching temperatures of 10–15 °C in the system while ambient temperatures are usually above 20 °C.

3.2. Experimental facility

The cycle's layout is a recuperated Rankine cycle due to the simplicity of the equipment involved and the necessary control infrastructure. The working fluid being in subcritical two-phase conditions allows for considerations on the vapor-liquid-equilibrium.

The setup of the test facility with measurement devices can be seen in Figs. 3 and 4 with the range of conditions shown in Table 4. The gaseous and liquid working fluid is present in the tank (State 0). Before entering the piston pump at State 1, it is subcooled with cold water. On the high-pressure side of the test facility, a strainer rids the working fluid of potential particles from construction or corrosion. The mass flow rate and density are measured at this position. The working fluid is preheated in the recuperator, a printed circuit heat exchanger, and then enters the primary heat exchanger for heat input. The flue gas is supplied by a gas burner operated with natural gas. At State 4, the working fluid is at its

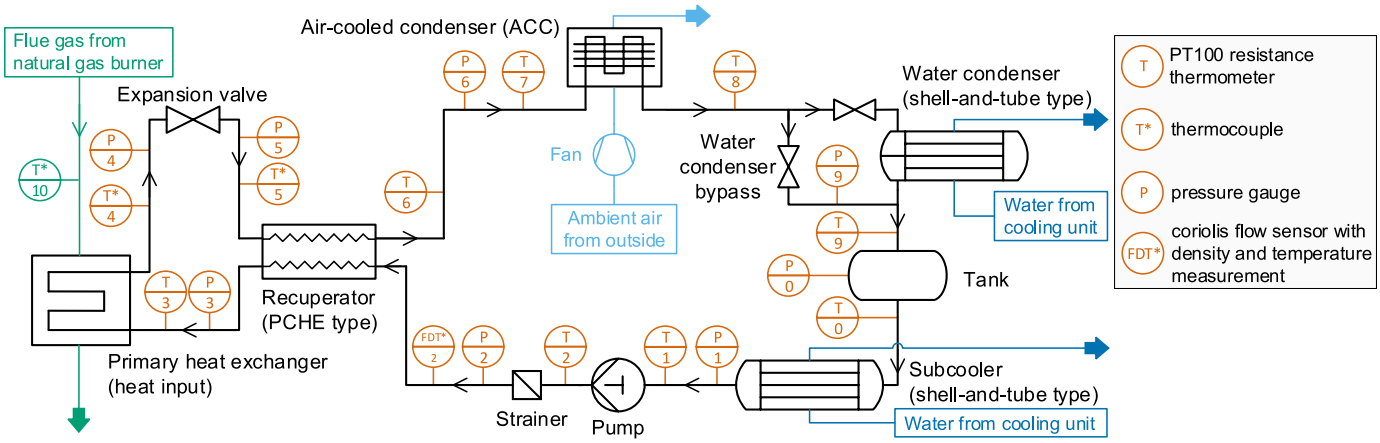

Fig. 3. Schematic view of the test facility.

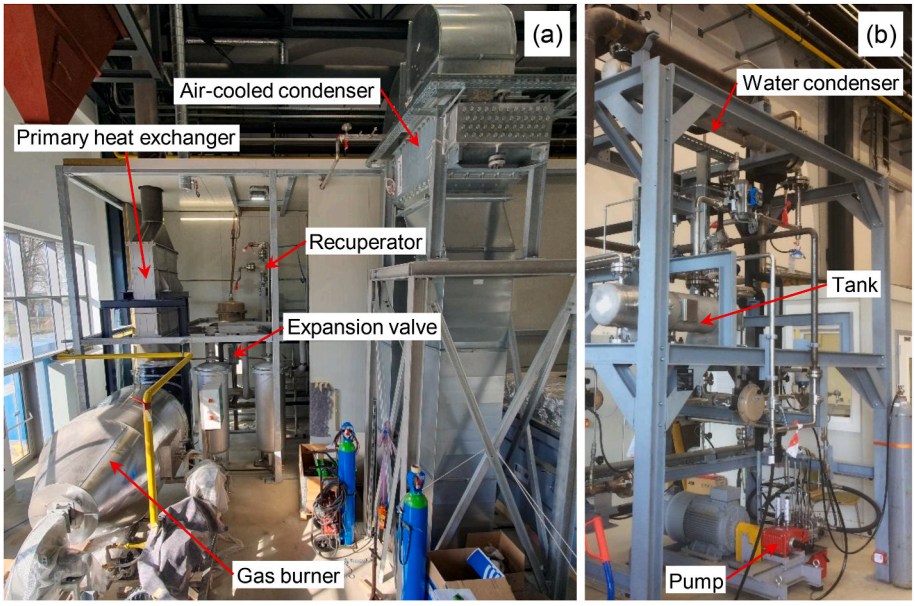

Fig. 4. Test facility during different stages of construction. (a) left part, (b) right part (behind air-cooled condenser and wall of picture (a)). The wall is part of a (now finished) fire-resistant safety installation.

Table 4
Operational range of key cycle parameters.

Parameter	Range (operational)
Heat source temperature/°C	50–830
Maximum pure CO_2 temperature/°C	600
Maximum mixture temperature/°C	507
Working fluid mass flow rate/kg/s	0.1-0.6
Low pressure/bar	45–98
High pressure/bar	80–135

highest temperature. Instead of a turbine, an expansion valve reduces the pressure in the system.[1] The working fluid enters the hot and low-pressure side of the recuperator at State 5. Pure CO_2 exits the recuperator overheated at State 6; the mixture is partially condensed due to restrictions in the maximum cycle temperature. Depending on the conditions of the working fluid and ambient airside, if the ACC is able to condense the flow, then the water condenser is bypassed. Otherwise, the working fluid is condensed to State 9. The condenser's duty/outlet temperature (control on temperature) determines the saturation pressure and, therefore, the low-pressure side.

Table 5 shows details of the experimental campaign with identifiers to match them to the presented data. The pure CO_2 experiments are for reference as the mixture properties introduce an uncertainty that the pure substance does not. Three sets of preliminary investigations were conducted on the low concentration mixture MX1.7 %. The goal was to test the filling concentration, a proof-of-concept and no signs of thermal degradation at elevated temperatures and to understand how reliable the vapor-liquid-equilibrium predicts the conditions on the low pressure side of the test facility. The MX6.2 % experiments showed the reliability of the mixture for a prolonged period of continuous operation, the robustness of the predicted properties and a deeper insight into the composition shift effect in power cycles with mixtures.

The filling method of the test facility worked thanks to the excellent mixing properties of CO_2 and C_6F_6: Filling in C_6F_6 first, and then CO_2

[1] The expansion valve was installed for budgetary reasons, as the scope of the funded project (mixtures and heat exchangers) was to demonstrate the concept and did not require a turbine. However, a valve is not a perfect replacement since the process sees a lower temperature reduction than that which a turbine would facilitate.

Table 5
Experimental campaign with purpose of testing and number of 2-min. steady-state measurement points; additional information on the experiments are documented in the repository.

ID	Date and Time	Working fluid	Purpose	Number of Measurement Points
E/CO2	8 individual days of experiments 27.07.23–14.09.23	pure CO_2	• **Reference** for comparisons (cycle conditions and property robustness in energy balance)	36
E/CO2/2	07.03.23 09:00–07.03.23 10:30	pure CO_2	• Vapor-liquid equilibrium test	8
e0	19.12.23 18:30–19.12.23 22:45	MX1.7 %	• Preliminary investigation: testing filling procedure • Proof of concept	19
e1	20.12.23 09:00–20.12.23 18:30	MX1.7 %	• **Proof of concept**: high temperature	9
e2	21.12.23 10:00–21.12.23 15:30	MX1.7 %	• Testing reliability of prediction of vapor-liquid equilibrium	19
E3	15.01.24 08:00–15.01.24 08:40	MX6.2 %	• Start-up (homogenization of working fluid)	/
E4	15.01.24 08:40–16.01.24 08:00	MX6.2 %	• Start-up and steady-state	6
E5	16.01.24 08:00–16.01.24 18:20	MX6.2 %	• Vapor-liquid equilibrium tests	18
E6	16.01.24 18:20–16.01.24 22:00	MX6.2 %	• Vapor-liquid equilibrium tests	14
E7	16.01.24 22:00–16.01.24 24:00	MX6.2 %	• Vapor-liquid equilibrium tests with varied high pressure	9
E8	17.01.24 00:00–17.01.24 04:00	MX6.2 %	• Increasing temperature for Proof-of-concept test	11
E9	17.01.24 04:00–17.01.24 07:00	MX6.2 %	• **Proof-of-concept** test at highest possible maximum temperature & at design and reduced mass flow rate	2
E10	17.01.24 07:00–17.01.24 16:00	MX6.2 %	• Steady-state, fixing broken sensor	1
E11	17.01.24 16:00–18.01.24 02:40	MX6.2 %	• Tests varying: high pressure, high temperature and mass flow rate	26
E12	18.01.24 02:40–18.01.24 07:15	MX6.2 %	• Vapor-liquid equilibrium tests varying: high pressure	6
E13	18.01.24 07:15–18.01.24 16:15	MX6.2 %	• Steady state	27
E14	18.01.24 16:15–18.01.24 22:30	MX6.2 %	• Vapor-liquid equilibrium tests varying: high pressure, mass flow rate	18
E15	18.01.24 22:30–19.01.24 11:15	MX6.2 %	• Air-cooled condenser testing varying: duty at fan; mass flow rates, low and high pressure	20
E16	19.01.24 11:15–19.01.24 18:00	MX6.2 %	• Air-cooled condenser testing varying: duty at fan; mass flow rates, low and high pressure	17
E17	19.01.24 18:00–20.01.24 18:30	MX6.2 %	• Steady state, Air-cooled condenser testing varying: duty at fan; mass flow rates, low and high pressure	19

Table 6
Fitted binary interaction parameters according to Ref. [48].

EoS	Value/formula	Comment
for PR	$k_{ij} = 0.163–0.000395T$	T in K
for PC-SAFT	$k_{ij} = 0.1023\text{-}0.0005574/(T/298.15)$	T in K

(instead of filling a pre-mixed composition). At the piston pump, small leakages occur, leading to a loss of working fluid over time.

The process control and data acquisition are conducted in a distributed control system. If not otherwise marked, the operating points in this study are 2-min mean values at steady-state. Further information on measurement devices and their uncertainties is available in the repository. We refrain from showing error bars indicating uncertainties to improve the figure readability.

3.3. Thermodynamic property models

The pure CO_2 properties are calculated as published by Span and Wagner [57] and realized via the software MATLAB.

For the calculation of the mixture vapor-liquid equilibrium, the Peng-Robinson (PR) equation with a quadratic mixing rule (van-der-Waals) was chosen after Di Marcoberardino et al.'s characterization based on their own and experimental data from the literature [48]. They fit the binary interaction parameter as a function of temperature, as reported in.

. The PR approach was chosen to find the current liquid composition based on the density ρ (at D2), temperature T (at FDT*2), and pressure p (at P2) measurement,[2] according to:

$$composition = f_{PR}(p, T, \rho) \quad (1)$$

All properties except VLE data were computed with the PC-SAFT (perturbated chain statistical associating fluid theory) with a fitted binary interaction parameter (see Table 6). The necessary pure component parameters were used as suggested by Di Marcoberardino et al. [17]. Although its VLE results are inferior to PR's, PC-SAFT was selected to calculate the other properties since it models the Helmholtz free energy, which allows for directly obtaining enthalpy, entropy, and specific heat.

For the property robustness analysis, an energy balance at the recuperator's high (HP) and low (LP) pressure side was calculated and compared, with the enthalpy calculated via PC-SAFT:

$$\dot{Q}_{LP} = -\dot{m}(h_6 - h_5) \quad (2)$$

$$\dot{Q}_{HP} = \dot{m}(h_2 - h_3) \quad (3)$$

$$h = f_{PC-SAFT}(composition, p, T) \quad (4)$$

With the mass flow rate $\dot{m}$ (measured at position F2), the composition (either filling composition or as calculated using Eq. (1)), the pressure p (at positions P2, P3, P5, P6), and the temperature T (at T*2, T3, T*5, and T6).

The software Aspen Plus V12.1 computed the mixture properties in a discretized manner. The fitting of discretized data and subsequent linear interpolation was performed in MATLAB.

3.4. Static equilibrium model for vapor-liquid-equilibrium

The "static equilibrium model" treats the test facility as a fixed volume filled with a constant mass of a certain filling concentration of CO_2/C_6F_6. The system is fully defined when assuming a uniform temperature distribution in the volume. Following this, all other conditions can be derived from the equilibrium data (correlation of temperature, pressure, and density for a fixed concentration) using the equation of state: pressure, gas and liquid phase compositions, and the amount of gas/

[2] For this composition-calculation approach, positioning of the Coriolis sensor FDT* would be even more beneficial at location 1 as the sensor would record the liquid density. In real life, this results in a pressure drop high enough to produce gas bubbles (and therefore a false, fluctuating density) and cavitation-like issues at the pump. The sensor is now located at position 2.

liquid. For the static equilibrium model, we use the Peng-Robinson EoS (see Section 3.3).

Given and resulting example conditions are indicated in Fig. 5. When dealing with a real system, three of the four conditions are already fixed (volume, mass, filling composition). For such a system, a direct relation exists between saturation pressure and saturation temperature. However, leakages might occur in a real system and influence the VLE [58].

As shown in Fig. 5, the gas phase of the system consists mainly of CO_2. In contrast, the liquid phase has a higher concentration of C_6F_6 than filling, which is favorable since the liquid phase is the relevant one as it constitutes the working fluid in the transcritical power cycle. Overall, a difference of liquid composition from the filling composition by 1 % occurs supporting the discussion reported in Section 2.2.

From the shape of the lens in the T,x,y-diagram in Fig. 5 (b), it is clear that the composition of the gas phase stays high in CO_2 for a wide range of conditions while the liquid composition undergoes a noticeable composition shift.

Fig. 5 (c) demonstrates the resulting conditions in the p,T-diagram: the resulting pressure/temperature condition lies in the two-phase region of the filling composition. The liquid composition's bubble and gas composition's dew-point line intersect at the resulting conditions.

A fixed volumetric system with a specific filling composition will be entirely filled with liquid when the liquid composition is the filling composition – which is the case at the filling composition's bubble line (dotted line in Fig. 6). Therefore, the phase boundary between the liquid and two-phase region is reached at the filling composition's bubble line: When more mass is in the system, the conditions are liquid (left of the bubble line), and with less mass, two phases are present. Due to the proximity of the operating point to the filling composition's bubble line, many authors approximate the correlation of condensation temperature/pressure with the bubble line [59].

A two-phase system of a fixed volumetric size filled with a certain composition without leakages undergoes changes in conditions along the lines of constant mass, as indicated by A- > B in Fig. 6. Moving to higher temperatures results in higher pressure and less of the higher-volatile (lower boiling point) component in the liquid. With increasing mass in the system, constant-mass- and constant-liquid-composition-lines become parallel because less vapor phase is in the system.

A leakage in the system leads to a movement away from the bubble line; lower pressures are the result when controlling the low-pressure side to the same temperature (vertical down-movement in Fig. 6).

Based on this understanding of the binary system, we discuss the results of the closed cycle in Section 4.4.

4. Results and discussion

4.1. Proof of concept and comparison to pure CO_2

In the proof-of-concept experiment with the MX1.7 % mixture, shown in Fig. 7, a maximum temperature of 507 °C was reached (at position T*4) at a mass flow rate of 0.4 kg/s and 100 bar on the high pressure side. The operation showed no signs of thermal degradation over the 19 h of testing – the VLE-results presented in Fig. 10 (recorded the day after the proof-of-concept of Fig. 7) showed the predicted correlations. A potential thermal degradation would influence the vapor-liquid-equilibrium significantly.

The T,s-diagram in Fig. 8 shows an example of comparable operating conditions of the mixture and pure CO_2 experiments.

For pure CO_2, the condensation at ~21 °C results in a condensation pressure of 61.5 bar. The low-pressure isobaric line of MX1.7 % has a similar slope trend while the working fluid condenses between 28 and 72 °C (temperature glide of 44 K) at 64.7 bar. Condensation in the recuperative heat exchanger occurs at the low-pressure side. Even though this condition is representative of CSP-optimized CO_2-mixture cycles [3], it was not accounted for in the design phase for the test facility. Potential risks are plug flow or flow instabilities, such as water hammer, but these did not occur.

A direct result of operating the cycle at a higher minimum temperature (see Fig. 8, MX6.2 %) is the increased low pressure – although this effect can be mitigated by using a higher concentration of C_6F_6 as it has a pure-substance critical pressure of 33 bar, which is lower than CO_2's. Consequently, using a mixture directly influences the pressure ratio and specific work of the cycle.

Slightly more heat is transferred by the recuperator using pure CO_2 and the MX6.2 % mixture. As the transferred heat is most sensitive to the temperature in condition 5 (high inlet temperature) and less so for pressure, a direct comparison without a detailed model accounting for the actual conditions in the heat exchanger is inconclusive. However, there is no significant indication of a penalized heat transfer using a mixture, which might have been expected due to an earlier condensation or higher resistance from the concentration change of the condensing mixture [60].

4.2. Solubility of additive (C_6F_6) in CO_2

The results confirm excellent solubility of C_6F_6 in CO_2: Fig. 9 shows the density measured after the pump. Before starting up the pump, the

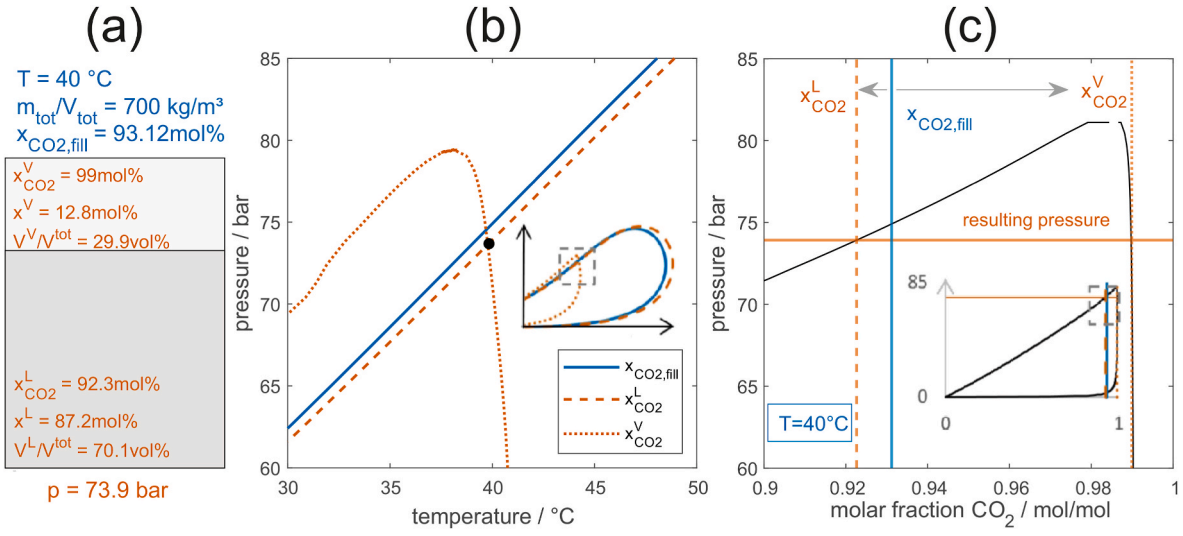

Fig. 5. Visualization of full equilibrium model, (a) inputs in blue, outputs in orange, (b) T,x,y-diagram, and (c) p,T-diagram of this system. (For interpretation of the references to colour in this figure legend, the reader is referred to the Web version of this article.)

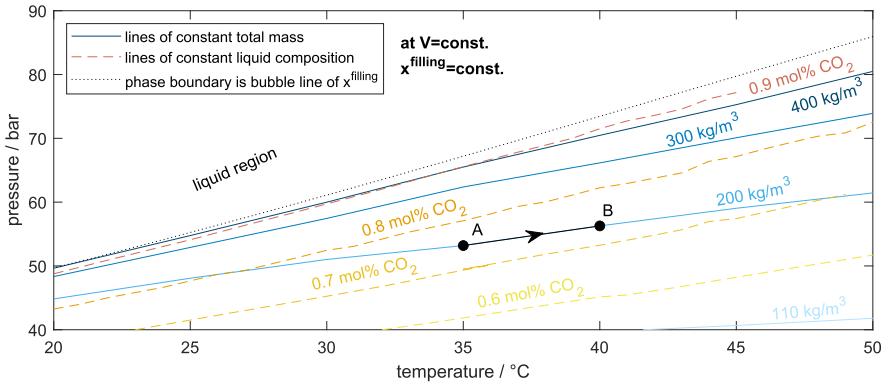

Fig. 6. p,T-diagram for a system with a fixed volume and filling composition of the zeotropic mixture CO_2/C_6F_6 based on the static equilibrium model.

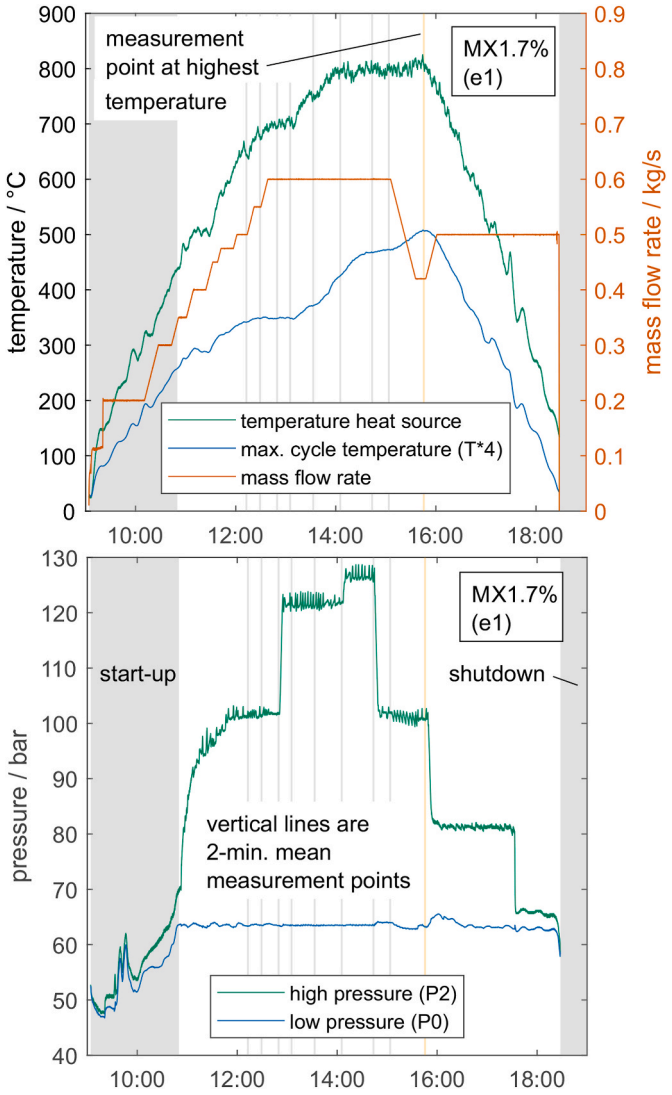

Fig. 7. Main cycle parameters over time of proof-of-concept experiment (e1) with CO_2/C_6F_6 mixture (MX1.7 %).

working fluid is gaseous at the density sensor (FDT*2). When the liquid reaches the sensor, the density increases, but the fluctuations indicate gas bubbles are present. The drop at 08:12 is recorded when the working fluid composition is richer in CO_2. Another slight decrease is visible with the bare eye but, after circulating through the test facility twice, the working fluid composition is homogenized.

The density trend over the full period of experiments stayed relatively constant with some deviation that could be traced back to composition shifts due to changed conditions in the cycle, which are discussed in Section 4.4. The two significant drops at day 3 were caused by the breakage of a temperature sensor that lead to a safety procedure allocating the cooling water to the condensers while shutting off the cooling of the pump, thus, leading to a temperature increase and drop in density.

4.3. Vapor-liquid equilibrium

The condensation at the cycle's low-pressure side determines the position of the transcritical cycle. The conditions at the tank of the cycle, measured by T9 and P0, represent the vapor-liquid-equilibrium. The pure CO_2 data points align well with the Span and Wagner prediction and also show the accuracy of the measurement devices involved, see Fig. 10.

Results from the mixture confirm the concept of the CO_2-based working fluids at a pilot scale and in a representative environment: The condensation pressure of the mixture is lower than for pure CO_2 and decreases for higher concentrations of C_6F_6. In both cases, MX1.7 % and MX6.2 %, the measured VLE data points are close to the approximate prediction: the bubble line (liquid saturation line). When comparing the Peng-Robinson to the PC-SAFT prediction, the higher concentration's prediction neatly overlaps while the lower shows a significant difference. This deviation could indicate that the actual filling concentration of MX1.7 % is lower but based on convergency issues at PC-SAFT phase boundaries of low C_6F_6 concentrations the authors do not deem this hypothesis reasonable.

The results from "MX6.2 %, water cond." (E10, E11) seem to lie at the bubble line of a lower C_6F_6 concentration, in contrast to the "MX6.2 %, ACC" (E7, E8). Besides the variation in controlled low-pressure side temperature T9, the only difference in the experiments is the duty of the in-series condensers. In (E10, E11), the condensation starts in the ACC (or even earlier, in the PCHE) and the water condenser condenses the flow to liquid conditions; whereas in (E7, E8), the water condenser is bypassed and the condensation fully completes in the ACC. The deviation between the experiments hints at a composition shift taking place, probably caused by the different hold-up of working fluid in the condensers. Section 4.4 expands on the composition shift using the PC-SAFT property method to calculate the composition's trends when process parameters are changed. However, the authors suggest using the Peng-Robinson method for predicting the VLE of the CO_2/C_6F_6 mixture because of the better fit at lower concentration.

4.4. Composition shift

The results in Fig. 11 show the concentration of the circulating fluid

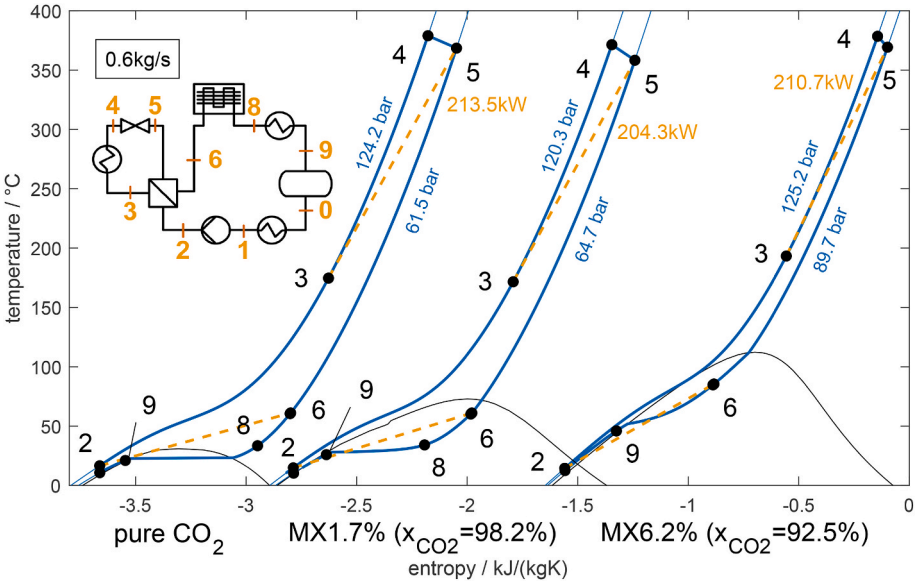

Fig. 8. T,s-diagrams of pure CO_2 and mixture operating conditions at design mass flow rate of 0.6 kg/s, exemplarily showing the conditions of a steady-state operation point of the experiments E/CO2, e1 and E8. Properties are shown for adjusted compositions.

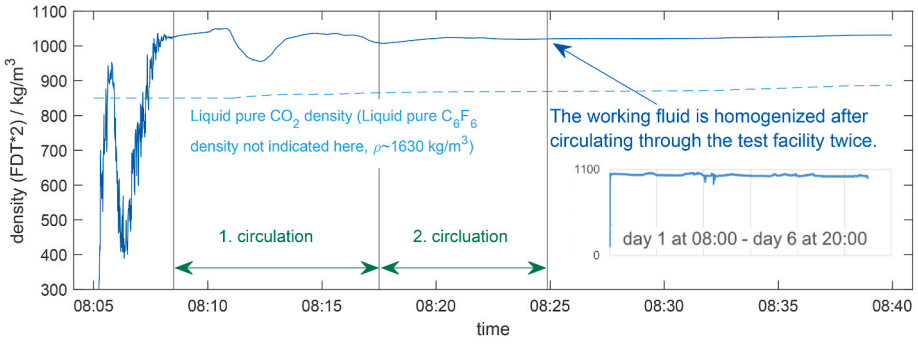

Fig. 9. Density of working fluid at start-up after filling test facility, experiment E3. P = 45–58 bar, T~11 °C. Diagram in right corner shows trend over the full time of continued operation.

as calculated after the pump (sensor FDT*2) as a function of temperature, pressure, and density. The concentration is close to the filling composition with an expected trend to higher C_6F_6 fractions at higher VLE pressures (and, subsequently, temperatures). It ranges from 6.4 to 8.4 % molar fraction of C_6F_6. The calculated concentrations show higher C_6F_6 concentrations than filling, as expected from fractionating. The results show higher concentration values (6.7–7.0 % C_6F_6) than were expected from the p,T-diagram of Fig. 10 (lower than filling concentration of 6.2 % C_6F_6). The range of concentrations is a magnitude higher than the uncertainty from filling.

During "VLE" experiments E5, E5, E16, the concentration uniquely correlates with the VLE conditions at the test facilities' low-pressure side, as the full equilibrium model suggests. The experiments have similar conditions throughout the test facility, as the high pressure and the supply temperature were controlled. The differences of E5, E6 and E16 are likely due to leakages as they were recorded at the beginning and the end of the prolonged operation (140h). The lost mass was also visible from the movement of the boundary layer/VLE, as it was matched by sensors T8 and T9 at different times during the experiments. The trend is consistent with the model from Fig. 6: at the same temperature, the earlier experiments (with a higher mass) show lower C_6F_6 concentrations. However, in the range of 7.25–7.6 % C_6F_6 fraction, two degrees of freedom (pressure and concentration) have the same trend while the temperature trend differs, which - assuming this model is correct - should then also follow the same trend. This might indicate the flaw in the model, the constant filling composition. With the leakage located at the pump, there is likely a loss of working fluid at the circulating concentration higher than the total (filling) composition, which means we deal with a changing overall concentration. Another possible explanation of the mismatch is that (neither) T8 or T9 pick up the exact VLE temperature due to the boundary layer being at different heights.

In "VLE, var. HP" experiments E2 and E7, the expansion valve position was fixed, allowing the high pressure to vary slightly. Especially at lower temperatures, E7, the results differ from E1, E11 experiments.

Four sets of experiments concerning the ACC, here depicted as "holdup", demonstrate the change of composition towards lower concentrations in the circulating fluid caused by an increased holdup in the condensers of the cycle. While controlling the VLE temperature (sensor T9 before the tank) via the amount of cooling water in the water condenser, the cooling power was shifted from the water condenser to the ACC by increasing the air volume flow, leading to lower temperatures in the ACC and therefore, a higher holdup of working fluid as more liquid already condenses there.

The "$T_{VLE,max}$" experiments (E8) show a seemingly stagnant concentration. Two opposed mechanisms may explain this behavior: The effect of the holdup is due to a higher pressure on the high-pressure part (P4) towards a lower C_6F_6 fraction balancing the effect of an increased VLE pressure and temperature, which shifts the composition to higher

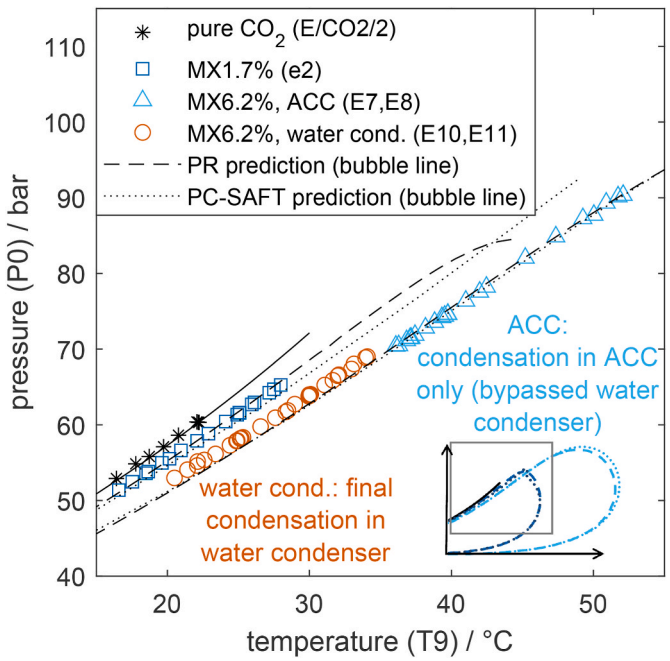

Fig. 10. p,T-diagram showing the VLE conditions at the low-pressure side of the test facility's tank for pure CO_2 and the mixtures. Dashed lines show the predicted bubble lines (liquid saturation lines) of the filling compositions and the saturation line for pure CO_2. There is a noticeable difference between the experiments with the water condenser and the ACC, hinting at a composition shift, probably caused by a different hold-up in the condensing heat exchangers (see next Section 4.4).

C_6F_6 fractions.

Consequences on the cycle are possible in off-design conditions but the effects self-stabilize the system. Higher condensation temperatures lead to a lower volatile (higher boiling point) circulating working fluid. This composition change is favorable and some authors even suggest "composition tuning" to match varying heat sink conditions by introducing a composition tuning sub system [61]. Increasing the condensation temperature means increasing the saturation pressure (low-pressure). With an additive whose critical pressure is lower than CO_2's, the pressure increase due to condensation temperature rise at the low-pressure side of the condensing cycle experiencing a compositions shift will be lower than in a system with a constant composition. From the turbine's perspective, an increased low pressure (back pressure of the turbine) in comparison to its design point will penalize its efficiency significantly [62]. The composition shift therefore also somewhat mitigates the high-condensation-temperature-penalty on the turbine's efficiency due to high back pressure. The composition shift will likely influence the heat transfer and lead to a different temperature distribution [63]. Since the properties only change slightly in reasonable ranges of composition shift (a few percentage points), we deem this effect small, unless a different heat transfer regime appears due to earlier condensation. When comparing the recuperator's duty for pure CO_2 and the mixtures, our results support this theory (see Fig. 8).

4.5. Property robustness analysis

Fig. 12 shows the energy balance of the recuperator. The pure CO_2 results in Fig. 12 (a) show excellent agreement between the high- and low-pressure sides at high transferred heat flows and a slightly worse but still good agreement at lower heat flows. The higher deviation at lower heat flows might be due to higher relative heat losses and, therefore, values for the low-pressure side heat that are too low.

The results for the mixtures also show a better agreement at a higher heat transferred. Starting from 150 kW, the results are within ± 10 %. Results of MX6.2 % below 80 kW are scattered. The MX1.7 % at small transferred heat (<60 kW) follows a clearer trend but significantly differs between the hot and cold side. The difference is not due to the properties calculated at the filling composition. Fig. 12 (b) shows the results with properties at the compositions derived in the previous section.

Comparing Fig. 12 (a) with (b), the results with adjusted composition follow a more cohesive, less scattered trend, supporting this correction which is necessary for obtaining performance-related information about the cycle. The discrepancy at lower transferred heat cannot be explained by heat losses or uncertainties since the pure CO_2 results do not support this theory. Instead, the trend hints at issues with the properties, probably at the low-pressure side where condensation happens and the enthalpy after the recuperator (state 6) was in the two-phase region.

5. Conclusions and future research

CO_2 blends offer a promising solution to enhancing power cycle conversion efficiency with respect to steam or sCO_2 cycles. This advantage is even more pertinent in the presence of dry cooling with high ambient temperatures which are typical locations of CSP plants. However, a working fluid constituted by two compounds might lead to operational issues such as composition shift and there was no experimental test facility operated at temperature above 300 °C to assess the

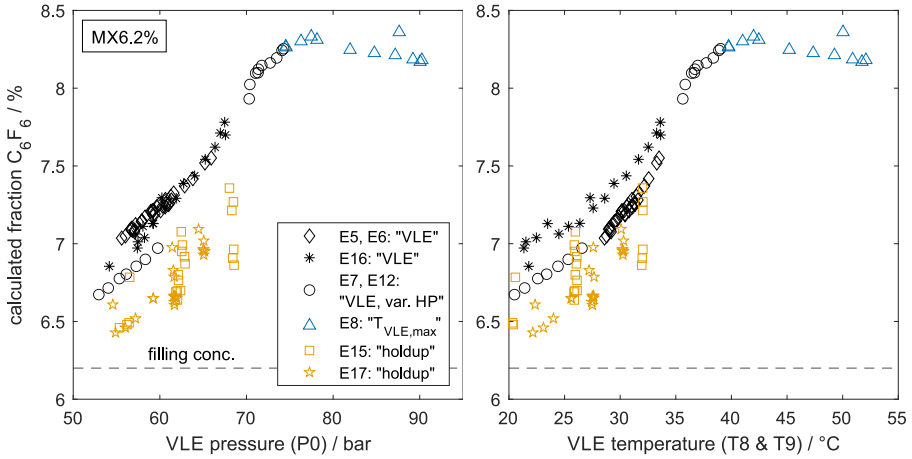

Fig. 11. Calculated concentration (Eq. (1)) of the circulating fluid over main operating conditions of the test facility. The results demonstrate that the static equilibrium model cannot represent the conditions – a holdup in various parts of the test facility has to be considered.

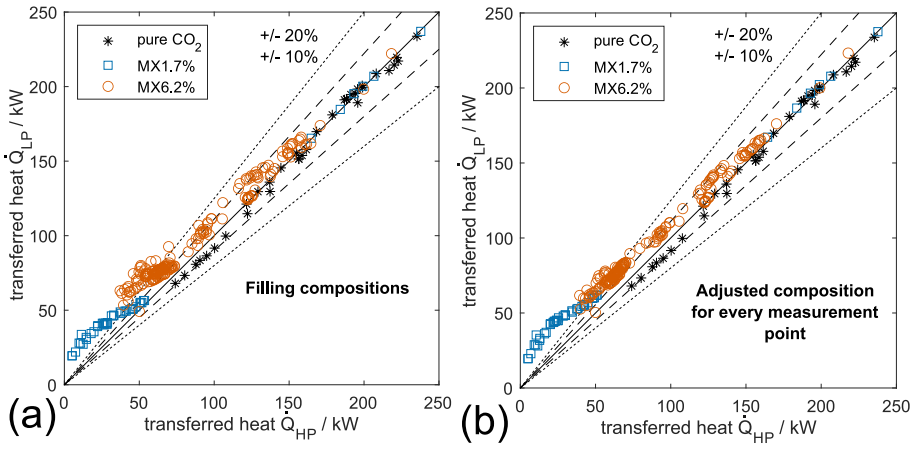

Fig. 12. Energy balance of recuperator. (a) calculated with filling composition, (b) calculated with adjusted composition.

impact of these potential issues. In the present study, the first recuperated Rankine cycle operating with a CO_2-based mixture up to temperatures of 500 °C in a relevant-sized setting has been presented. Among the proposed working fluids in literature, CO_2/C_6F_6 is selected for the experimental campaign considering two different mixture compositions: 98.3 %/1.7 % and 93.8 %/6.2 % (molar fractions). The cumulative 170 h of operation confirm the soundness of the proposed concept as no issues arose during the operation.

The prediction of the vapor-liquid equilibrium via minimally fitted EoS – namely Peng-Robinson – was confirmed as accurate, and the experimental data at the low-pressure side of the test facility correspond well with the predicted for most operating conditions.

However, the working fluid showed a significant composition shift due to several effects.

1. gas and liquid separation,
2. varied temperature control at the low-pressure side,
3. varied cycle conditions (maximum cycle conditions, liquid holdup).

A composition shift was shown experimentally by observing density shifts that experience an expected behavior at the change of operating conditions in the system. As a consequence, the correlation between saturation conditions at the low-pressure side of the cycle, temperature and pressure, do not (in all conditions) follow the bubble line of the mixture's filling composition. The concentration shifts favor the CO_2-based-mixture-concept and mitigate efficiency penalties at high condensation temperatures because higher condensation temperatures lead to a lower volatile (higher boiling point) circulating working fluid. The gas phase is almost pure CO_2, while a higher-than-filling concentration of the lower volatile (high boiling point) C_6F_6 constitutes the liquid phase which is circulating the cycle. Changing the temperature at the low-pressure side, as could happen during the day when heat rejection is accomplished with ambient air, results in a composition shift. At higher condensation temperatures (and the corresponding higher condensation pressures), the circulating fluid contains more C_6F_6 (lower volatile/high boiling point component). Cycle conditions at the high-pressure side, such as high pressure or maximum temperature, lead to a composition shift. A higher holdup of liquid in the condensers caused by a different temperature profile along the condensers, while maintaining the condensation temperature control, results in the working fluid having a lower concentration of C_6F_6.

A simple VLE model, here referred to as a static-equilibrium-model, which represents the whole test facility as a volume where the gas phase is in full equilibrium with all the liquid and circulating working fluid, could not predict the measured VLE conditions. This inadequate correlation means the working fluid experiences a pseudo-equilibrium at the gas-liquid boundary layer in the tank. Future research must provide a sound and accessible model for the design process to predict the composition shifts. So far, only detailed models that have solely been verified with insufficient data and are based on discretized heat exchanger models relying on heat transfer correlations are available.

Using operational data (temperature, pressure, density) to determine the composition based on EoS-predictions is a fast and inexpensive way of monitoring the current composition that only requires a Coriolis sensor and look-up tables.

For analysis and, subsequently, for design and operational optimization, knowledge of the circulating fluid's composition is vital since the saturation conditions will directly impact a turbine. A closer look into heat transfer effects due to a shifted composition is necessary to understand the impact on a real system. Due to the rare use of C_6F_6, its properties and especially properties in the mixture with CO_2 are not abundantly available and will need to be assessed before conducting deeper investigations.

The selection of the additive to the CO_2-based working fluid needs more attention, accounting for the CO_2/SO_2 mixture's thermal stability in comparison to CO_2/C_6F_6, and thus, whether it can further exploit the benefits of the proposed cycle despite the additional safety issues.

CRediT authorship contribution statement

Viktoria Carmen Illyés: Writing – original draft, Visualization, Methodology, Formal analysis, Conceptualization. **Gioele Di Marcoberardino:** Writing – review & editing. **Andreas Werner:** Writing – review & editing, Supervision, Project administration. **Markus Haider:** Resources, Funding acquisition. **Giampaolo Manzolini:** Writing – review & editing, Funding acquisition.

Declaration of competing interest

The authors declare that they have no known competing financial interests or personal relationships that could have appeared to influence the work reported in this paper.

Acknowledgements

The SCARABEUS project has received funding from European Union's Horizon 2020 research program under grant agreement N°814985.

The authors acknowledge TU Wien Bibliothek for financial support through its Open Access Funding Program.

The authors acknowledge TU Wien Bibliothek for financial support for editing/proofreading.

Data availability

Data for this article, including•
P&ID diagram and information about sensors•
Raw measurement data•
Thermodynamic models (Example Aspen Plus files)•
Thermodynamic data produced by models via Aspen Plus•
Analysis (Software files (MATLAB) including property tables)

are available at Zenodo, see DOI: https://doi.org/10.5281/zenodo.13170843.

References

[1] He Y-L, et al. Perspective of concentrating solar power. Energy May 2020;198:117373. https://doi.org/10.1016/j.energy.2020.117373.
[2] Dostal V, Hejzlar P, Driscoll MJ. The supercritical carbon dioxide power cycle: comparison to other advanced power cycles. Nucl Technol Jun. 2006;154(3):283–301. https://doi.org/10.13182/NT06-A3734.
[3] Crespi F, et al. Thermal efficiency gains enabled by using CO2 mixtures in supercritical power cycles. Energy Jan. 2022;238:121899. https://doi.org/10.1016/j.energy.2021.121899.
[4] Liqreina A, Qoaider L. Dry cooling of concentrating solar power (CSP) plants, an economic competitive option for the desert regions of the MENA region. Sol Energy May 2014;103:417–24. https://doi.org/10.1016/j.solener.2014.02.039.
[5] Angelino G, Invernizzi C. Real gas Brayton cycles for organic working fluids. Proc Inst Mech Eng Part J Power Energy Feb. 2001;215(1):27–38. https://doi.org/10.1243/0957650011536543.
[6] Manzolini G, Binotti M, Bonalumi D, Invernizzi C, Iora P. CO2 mixtures as innovative working fluid in power cycles applied to solar plants. Techno-economic assessment. Sol Energy Mar. 2019;181:530–44. https://doi.org/10.1016/j.solener.2019.01.015.
[7] Yang Z, et al. Analysis of lower GWP and flammable alternative refrigerants. Int J Refrig Jun. 2021;126:12–22. https://doi.org/10.1016/j.ijrefrig.2021.01.022.
[8] Abedini H, et al. A comprehensive analysis of binary mixtures as working fluid in high temperature heat pumps. Energy Convers Manag Feb. 2023;277:116652. https://doi.org/10.1016/j.enconman.2022.116652.
[9] Guo H, Gong M, Qin X. Performance analysis of a modified subcritical zeotropic mixture recuperative high-temperature heat pump. Appl Energy Mar. 2019;237:338–52. https://doi.org/10.1016/j.apenergy.2018.12.094.
[10] Conboy T, Wright S, Ames D, Lewis T. CO2-based mixtures as working fluids for geothermal turbines. Jan. 2012. https://doi.org/10.2172/1049477. SAND2012-4905, 1049477.
[11] Modi A, Haglind F. A review of recent research on the use of zeotropic mixtures in power generation systems. Energy Convers Manag Apr. 2017;138:603–26. https://doi.org/10.1016/j.enconman.2017.02.032.
[12] Lasala S, Bonalumi D, Macchi E, Privat R, Jaubert J-N. The design of CO 2 -based working fluids for high-temperature heat source power cycles. Energy Proc Sep. 2017;129:947–54. https://doi.org/10.1016/j.egypro.2017.09.125.
[13] Crespi F, Rodríguez De Arriba P, Sánchez D, Muñoz A. Preliminary investigation on the adoption of CO 2 -SO 2 working mixtures in a transcritical Recompression cycle. Appl Therm Eng Jul. 2022;211:118384. https://doi.org/10.1016/j.applthermaleng.2022.118384.
[14] Morosini E, Ayub A, Di Marcoberardino G, Invernizzi CM, Iora P, Manzolini G. Adoption of the CO2 + SO2 mixture as working fluid for transcritical cycles: a thermodynamic assessment with optimized equation of state. Energy Convers Manag Mar. 2022;255:115263. https://doi.org/10.1016/j.enconman.2022.115263.
[15] Crespi F, Martínez GS, Rodriguez De Arriba P, Sánchez D, Jiménez-Espadafor F. Influence of working fluid composition on the optimum characteristics of blended supercritical carbon dioxide cycles, vol. 10. American Society of Mechanical Engineers; Jun. 2021, V010T30A030. https://doi.org/10.1115/GT2021-60293. *Supercritical CO2*, Virtual, Online.
[16] Manzolini G, et al. Adoption of CO2 blended with C6F6 as working fluid in CSP plants. In: Presented at the SOLARPACES 2020: 26th international conference on concentrating solar power and chemical energy systems; 2022, 090005. https://doi.org/10.1063/5.0086520. Freiburg, Germany.
[17] Di Marcoberardino G, Morosini E, Manzolini G. Preliminary investigation of the influence of equations of state on the performance of CO2 + C6F6 as innovative working fluid in transcritical cycles. Energy Jan. 2022;238:121815. https://doi.org/10.1016/j.energy.2021.121815.
[18] Abbas SM, Alhassany HDS, Vera D, Jurado F. Review of enhancement for ocean thermal energy conversion system. J Ocean Eng Sci Oct. 2023;8(5):533–45. https://doi.org/10.1016/j.joes.2022.03.008.
[19] Li D, Yin G, Gao W, Zhang C. Role of CO2-based mixtures in the organic Rankine cycle using LNG cold energy. Sustain. Energy Technol. Assess. May 2024;65:103752. https://doi.org/10.1016/j.seta.2024.103752.
[20] McLinden MO, Huber ML. (R)Evolution of refrigerants. J Chem Eng Data Sep. 2020;65(9):4176–93. https://doi.org/10.1021/acs.jced.0c00338.
[21] Sosa JE, et al. Adsorption of fluorinated greenhouse gases on activated carbons: evaluation of their potential for gas separation. J Chem Technol Biotechnol Jul. 2020;95(7):1892–905. https://doi.org/10.1002/jctb.6371.
[22] Kalina AI. Combined-cycle system with novel bottoming cycle. J Eng Gas Turbines Power Oct. 1984;106(4):737–42. https://doi.org/10.1115/1.3239632.
[23] Angelino G, Colonnadipaliano P. Multicomponent working fluids for organic rankine cycles (ORCs). Energy Jun. 1998;23(6):449–63. https://doi.org/10.1016/S0360-5442(98)00009-7.
[24] Heberle F, Preißinger M, Brüggemann D. Zeotropic mixtures as working fluids in Organic Rankine Cycles for low-enthalpy geothermal resources. Renew Energy Jan. 2012;37(1):364–70. https://doi.org/10.1016/j.renene.2011.06.044.
[25] Demuth OJ. Analyses of mixed-hydrocarbon binary thermodynamic cycles for moderate-temperature geothermal resources. Feb. 1981. https://doi.org/10.2172/6889398. EGG-PG-G-80-041, 6889398.
[26] Bamorovat Abadi G, Kim KC. Investigation of organic Rankine cycles with zeotropic mixtures as a working fluid: advantages and issues. Renew Sustain Energy Rev Jun. 2017;73:1000–13. https://doi.org/10.1016/j.rser.2017.02.020.
[27] REGULATION (EU). 2024/573 OF THE EUROPEAN PARLIAMENT AND OF THE COUNCIL on fluorinated greenhouse gases, amending Directive (EU) 2019/1937 and repealing Regulation (EU) No 517/2014. 2024. https://doi.org/10.5040/9781782258674.
[28] Wang JL, Zhao L, Wang XD. A comparative study of pure and zeotropic mixtures in low-temperature solar Rankine cycle. Appl Energy Nov. 2010;87(11):3366–73. https://doi.org/10.1016/j.apenergy.2010.05.016.
[29] Jung H-C, Taylor L, Krumdieck S. An experimental and modelling study of a 1 kW organic Rankine cycle unit with mixture working fluid. Energy Mar. 2015;81:601–14. https://doi.org/10.1016/j.energy.2015.01.003.
[30] Li T, Zhu J, Fu W, Hu K. Experimental comparison of R245fa and R245fa/R601a for organic Rankine cycle using scroll expander. Int J Energy Res 2015;39:202–14. https://doi.org/10.1002/er.3228.
[31] Bamorovat Abadi G, Yun E, Kim KC. Experimental study of a 1 kw organic Rankine cycle with a zeotropic mixture of R245fa/R134a. Energy Dec. 2015;93:2363–73. https://doi.org/10.1016/j.energy.2015.10.092.
[32] Wang Y, Liu X, Ding X, Weng Y. Experimental investigation on the performance of ORC power system using zeotropic mixture R601a/R600a: ORC power system using R601a/R600a. Int J Energy Res Apr. 2017;41(5):673–88. https://doi.org/10.1002/er.3664.
[33] Blondel Q, Tauveron N, Caney N, Voeltzel N. Experimental study and optimization of the organic rankine cycle with pure NovecTM649 and zeotropic mixture NovecTM649/hfe7000 as working fluid. Appl Sci May 2019;9(9):1865. https://doi.org/10.3390/app9091865.
[34] Cai J, Shu G, Tian H, Wang X, Wang R, Shi X. Validation and analysis of organic Rankine cycle dynamic model using zeotropic mixture. Energy Apr. 2020;197:117003. https://doi.org/10.1016/j.energy.2020.117003.
[35] Huang X, Zhang J, Haglind F. Experimental analysis of high temperature flow boiling of zeotropic mixture R134a/R245fa in a plate heat exchanger. Appl Therm Eng Feb. 2023;220:119652. https://doi.org/10.1016/j.applthermaleng.2022.119652.
[36] Lu P, et al. Experimental investigation of a zeotropic organic Rankine cycle system with liquid-separation condensation for composition adjustment. Energy Convers Manag Oct. 2023;293:117540. https://doi.org/10.1016/j.enconman.2023.117540.
[37] Wang Z, Zhao Y, Xia X, Pan H, Zhang S, Liu Z. Experimental evaluation of organic Rankine cycle using zeotropic mixture under different operation conditions. Energy Feb. 2023;264:126188. https://doi.org/10.1016/j.energy.2022.126188.
[38] Shu G, Yu Z, Tian H, Liu P, Xu Z. Potential of the transcritical Rankine cycle using CO2-based binary zeotropic mixtures for engine's waste heat recovery. Energy Convers Manag Oct. 2018;174:668–85. https://doi.org/10.1016/j.enconman.2018.08.069.
[39] About Desolination. [Online]. Available: https://desolination.eu/about-the-project/.
[40] Petruccelli G, Turunen-Saaresti T, Grönman A, Lugo A. Study on the operation of the LUTsCO2 test loop with pure CO2 and CO2 + SO2 mixture through dynamic modeling. In: Proceedings of the 4th international seminar on non-ideal compressible fluid dynamics for propulsion and power, in ERCO, vol. 29. Springer Nature Switzerland AG; 2023. p. 191–200. https://doi.org/10.1007/978-3-031-30936-6_19 [Online]. Available:.
[41] Chen J, Kruse H. Concentration shift simulation for the mixed refrigerants R-404a, R-32/134a, and R-407C in an air conditioning system. HVAC R Res Apr. 1997;3(2):149–57. https://doi.org/10.1080/10789669.1997.10391368.
[42] Zhao L, Bao J. The influence of composition shift on organic Rankine cycle (ORC) with zeotropic mixtures. Energy Convers Manag Jul. 2014;83:203–11. https://doi.org/10.1016/j.enconman.2014.03.072.
[43] Xu X, Liu J, Cao L, Li Z. Local composition shift of mixed working fluid in gas–liquid flow with phase transition. Appl Therm Eng Jun. 2012;39:179–87. https://doi.org/10.1016/j.applthermaleng.2012.01.064.
[44] Morosini E, et al. Off-design of a CO2-based mixture transcritical cycle for CSP applications: analysis at part load and variable ambient temperature. Appl Therm Eng Jan. 2024;236:121735. https://doi.org/10.1016/j.applthermaleng.2023.121735.
[45] U.S. Secretary of Commerce, "Hexafluorobenzene, NIST Chemistry WebBook." NIST Standard Reference Data. Accessed: September. 30, 2024. [Online]. Available: https://webbook.nist.gov/cgi/inchi?ID=C392563&Mask=4.
[46] Yaws CL, Li KY, Kuo CH. Sulfur oxides: SO2, SO3. Chem Eng 1974;85:85–92.
[47] U.S. Secretary of Commerce, "Titanium tetrachloride, NIST Chemistry WebBook." NIST Standard Reference Data. Accessed: September. 30, 2024. [Online]. Available: https://webbook.nist.gov/cgi/cbook.cgi?ID=C7550450&Mask=4.
[48] Di Marcoberardino G, et al. Experimental characterisation of CO2 + C6F6 mixture: thermal stability and vapour liquid equilibrium test for its application in

transcritical power cycle. Appl Therm Eng Jul. 2022;212:118520. https://doi.org/10.1016/j.applthermaleng.2022.118520.
[49] Weil ED, Sandler SR. Sulfur compounds. In: Othmer Kirk-, editor. Kirk-othmer encyclopedia of chemical technology. first ed. Wiley; 2000. https://doi.org/10.1002/0471238961.1921120623050912.a01.
[50] Orellano P, Reynoso J, Quaranta N. Short-term exposure to sulphur dioxide (SO2) and all-cause and respiratory mortality: a systematic review and meta-analysis. Environ Int May 2021;150:106434. https://doi.org/10.1016/j.envint.2021.106434.
[51] Verordnung des Bundesministers für Arbeit über Grenzwerte für Arbeitsstoffe sowie über krebserzeugende und fortpflanzungsgefährdende (reproduktionstoxische) Arbeitsstoffe (Grenzwerteverordnung 2021 – GKV). [Online]. Available: https://www.ris.bka.gv.at/eli/bgbl/II/2007/243/20070911.
[52] Kapias T, Griffiths R. Accidental releases of titanium tetrachloride (TiCl) in the context of major hazards?spill behaviour using REACTPOOL. J Hazard Mater Mar. 2005;119(1–3):41–52. https://doi.org/10.1016/j.jhazmat.2004.12.001.
[53] Murray E, Llados F. Toxicological profile for titanium tetrachloride. U.S. DEPARTMENT OF HEALTH AND HUMAN SERVICES, Public Health Service Agency for Toxic Substances and Disease Registry; 1997.
[54] European Chemicals Agency, "Substance Infocard. Hexafluorobenzene." Accessed: August. 4, 2024. [Online]. Available: https://echa.europa.eu/substance-information/-/substanceinfo/100.006.252.
[55] reportScientific assessment of Ozone depletion: 2022. Geneva: World Meteorological Organization (WMO); 2022. GAW Report No. 278.
[56] abcr GmbH. Offer hexafluorobenzene. 2023.
[57] Span R, Wagner W. A new equation of state for carbon dioxide covering the fluid region from the triple-point temperature to 1100 K at pressures up to 800 MPa. J Phys Chem Ref Data 1996;25(6):1509–96. https://doi.org/10.1063/1.555991.
[58] Johansson A, Lundqvist P. A method to estimate the circulated composition in refrigeration and heat pump systems using zeotropic refrigerant mixtures. Int J Refrig 2001;24(8):798–808. https://doi.org/10.1016/S0140-7007(00)00061-X.
[59] Liu Q, Duan Y, Yang Z. Effect of condensation temperature glide on the performance of organic Rankine cycles with zeotropic mixture working fluids. Appl Energy 2014;115:394–404. https://doi.org/10.1016/j.apenergy.2013.11.036.
[60] Del Col D, Azzolin M, Bortolin S, Zilio C. Two-phase pressure drop and condensation heat transfer of R32/R1234ze(E) non-azeotropic mixtures inside a single microchannel. Sci. Technol. Built Environ. Jul. 2015;21(5):595–606. https://doi.org/10.1080/23744731.2015.1047718.
[61] Collings P, Yu Z, Wang E. A dynamic organic Rankine cycle using a zeotropic mixture as the working fluid with composition tuning to match changing ambient conditions. Appl Energy Jun. 2016;171:581–91. https://doi.org/10.1016/j.apenergy.2016.03.014.
[62] Illyés V, et al. Dry-cooled rankine cycle operated with binary carbon dioxide based working fluids. SolarPACES Conf. Proc. Apr. 2024;1. https://doi.org/10.52825/solarpaces.v1i.625.
[63] Zhou Y, Zhang F, Yu L. The discussion of composition shift in organic Rankine cycle using zeotropic mixtures. Energy Convers Manag May 2017;140:324–33. https://doi.org/10.1016/j.enconman.2017.02.081.